Spectrogram approach to S^2 fiber mode analysis to distinguish between dispersion and distributed scattering

J. Jasapara* and A. D. Yablon

Interfiber Analysis, LLC, 26 Ridgewood Drive, Livingston, New Jersey 07039, USA
*Corresponding author: jasapara@interfiberanalysis.com

We report on the significant effect that intermodal dispersion can have on spatially and spectrally resolved interferometric (S^2) fiber mode analysis. This dispersion can significantly broaden the measured intermodal group delay and could be misinterpreted as distributed scattering. In our new approach, the spectral interference data is analyzed over multiple wavelength windows staggered across the measurement bandwidth and assembled together to form a spectrogram that reveals the wavelength dependence of the intermodal group delay. Measurements on standard telecom single-mode and large-mode-area fibers are presented. This spectrogram analysis is a more accurate map of mode conversion along the fiber and is essential for evaluating fibers and fiber devices.   © 2012 Optical Society of America

OCIS codes: 060.2270, 060.2320.

Spatially resolved spectral interferometry (S^2) [1–3] is one approach (see also [4]) to characterize the energy exchanged between modes in multi-mode fibers based on the inter-modal group delay between the various guided modes and the dominant mode, which is usually the fundamental mode. Spatially and spectrally resolved interferometry is powerful not only because it provides the relative power and spatial distribution of the excited modes, but also because it provides insight into whether those modes are excited at discrete or distributed locations within the fiber. For this reason, S^2 is an important tool to evaluate fibers used in fiber lasers/amplifiers [5], sensors, or telecom systems [6].

A narrow spike in the S^2 intermodal group delay spectrum indicates a discrete excitation of a higher-order-mode (HOM). Previously [1], a broad distribution in inter-modal group delay was assumed to be distributed mode excitation in the fiber. However, the effects of intermodal dispersion on the measurement have not been accounted for in the current literature. We have discovered that the fiber's dispersion can also cause a discrete scattering event to manifest itself as a broad distribution in the intermodal group delay. For example, fibers designed for lasers that have low numerical apertures can weakly guide HOMs with strong waveguide dispersion.

In this Letter, we describe a new approach to S^2 data analysis, which resolves the ambiguity associated with broadened distributions in the intermodal group delay maps. The data is analyzed over small staggered wavelength windows across the measurement bandwidth and assembled together to form a map of the intermodal group delay as a function of wavelength—we call this map a *spectrogram*. The wavelength dependence of the intermodal group delay manifests itself as an inclination in streaks traversing the spectrogram. This new two-dimensional perspective resolves the ambiguity as to whether group delay broadening is caused by fiber dispersion or distributed scattering that is inherent to the previous one-dimensional S^2 mapping [1–3]. Results for a standard telecom single-mode fiber and a large-mode-area (LMA) fiber are presented.

The experimental setup used to capture the spatial dependence of spectral interferograms of fiber near-field images is shown in Fig. 1. A narrow line-width laser (line-width ≤ 130 kHz) tunable from 1000 to 1066 nm is launched into the fiber under test. The output end of this fiber is imaged onto a silicon CCD camera, which captures the images as the laser wavelength is scanned across its ~66 nm span. The camera pixel size was approximately 6×6 μm. A 100×100 pixel area was sufficient to capture the magnified near field images.

The laser output is attenuated and effectively polarized by two reflections off glass wedges near Brewster's angle of incidence that direct the beam to the camera (not shown in Fig. 1). The near-field images captured by the camera as a function of laser wavelength are analyzed with a computer.

We first studied a 20 m long 125 μm cladding diameter LMA passive fiber containing a 20 μm diameter core with a numerical aperture of 0.08. The fiber modes and their group effective index were calculated using a scalar model from a refractive index profile measured by a fiber analyzer (IFA-100, Interfiber Analysis, LLC) at a wavelength of 1000 nm. The scalar model showed that the LP_{01}, LP_{11}, LP_{02}, and LP_{12} HOMs were guided by this fiber.

The multi-mode fiber was spliced to the single-mode output pigtail from the laser. It was arranged in ~25 cm diameter loose coils to prevent any bend induced perturbations that may cause mode scattering. Under these conditions the coupling into the fiber is axisymmetric and, therefore, only the even LP_{02} HOM was observed at the output. A 20 g weight was placed just downstream of the splice to introduce a discrete nonaxisymmetric perturbation that could excite odd modes.

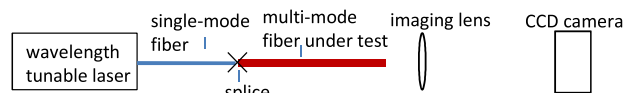The laser wavelength was scanned and near-field images of the fiber's output end face were captured as

Fig. 1.   (Color online) Schematic of the experimental setup.

a function of laser wavelength. Following the standard S^2 analysis [1,2], the Fourier transform of the spectral interference pattern at each pixel was calculated. The transform gives the Fourier amplitude of the intermodal beats as a function of intermodal group delay.

A sum of the Fourier transforms over all the pixels is shown in Fig. 2(a). The Fourier amplitudes can be related to the relative strengths of the beating modes [1]. We verified that peaks S1, S2, and S3 were also present in separate measurements on a single mode fiber and were therefore caused by known reflections within our experimental setup—they should thus be ignored. By analyzing the spatial dependence of the Fourier phase and amplitude at an intermodal group delay point, the phase and energy distribution of the mode contributing at that delay can be reconstructed. Reconstruction of the Fourier phase and intensity images at the narrow peak D reveals that it corresponds to discrete scattering into the LP_{11} mode. This mode is excited at the localized perturbation caused by the weight because it appears only when the weight is introduced.

Figure 2(a) also shows a broad distribution in intermodal group delay over regions X1 and X2. Reconstruction of the Fourier phase and intensity over these regions shows that it substantially consists of the LP_{02} mode. According to the standard S^2 interpretation [1–3], these broadened delay distributions, X1 and X2, show light coupling from the LP_{01} to the LP_{02} mode over a long length, i.e., the fiber causes distributed scattering from the LP_{01} mode into the LP_{02} mode. This interpretation

overlooks the group delay dispersion that is often substantial near the mode cutoff of HOMs and therefore falsely identifies the fiber or its fixturing as the excitation source of the HOMs.

The dispersion and distributed scattering effects are decoupled by our new analysis method. The S^2 data is collected as described above. However, when analyzing the data, we take a narrow wavelength window and sweep it across the full laser spectrum in small wavelength steps. We create a spectrogram by summing the Fourier transforms at all pixels over these windows and stacking them together to form a two-dimensional image that shows the Fourier amplitude as a function of the intermodal group delay on one axis and the center wavelength of the window on the other axis. Figure 2(b) shows such a spectrogram recorded with the LMA fiber. We used ~8 nm wide spectral windows with a step size of 2 nm. The spectral width is chosen so that the peaks are resolved in intermodal group delay whereas the step size is chosen to capture the wavelength-dependence of the spectrogram features. The MPI within each wavelength window can be calculated according to the algorithm in [1] for a wavelength-dependent MPI. The window parameters do not affect the MPI values.

The spectrogram has several interesting features. Most importantly we see that the broad delay features X1 and X2 in Fig. 2(a) appear as a single curved streak X in the spectrogram indicating a strong variation of the intermodal group delay from ~13 ps to ~33 ps across the laser tuning range. The insets in Fig. 2(b) show reconstructions of the intensity profile at a few delays along streak X and indicate an LP_{02} mode. On the other hand, peak D in Fig. 2(a) corresponds to a streak with relatively little variation in delay across the laser tuning range indicating that the LP_{11} mode experiences weak intermodal dispersion. Reconstruction of the LP_{11} mode at a couple of points along streak D are shown as insets in Fig. 2(b). This spectrogram correctly identifies that the spread of LP_{02} intermodal group delay [features X1 and X2 in Fig. 2(a)] is actually caused by intermodal fiber dispersion acting on a discrete scattering event at the input splice rather than distributed scattering in the fiber. The theoretical spectrogram was simulated from the calculated group indices. The wavelength dependence of intermodal group delay features X and D [Fig. 2(c)] are in good qualitative agreement with the measured data.

In addition, an inflected streak B is present in both the measured and simulated spectrograms [Figs. 2(b) and 2(c)]. Reconstruction of the mode intensity along feature B shows a clear mixture of the LP_{11} and LP_{02} modes [see inset of Fig. 2(b)]. Therefore, feature B arises from the beating of the LP_{11} mode against the LP_{02} mode and the delay values represent the magnitude of intermodal group delay between these two HOMs as a function of wavelength—this is equivalent to the magnitude of the intermodal group delay difference between the trajectories of streaks X and D. Other faint streaks are visible that represent interaction of the fundamental mode with spurious reflections (peaks S1, S2, and S3) in our setup. Although they affect the accuracy of an MPI computation, they are specific to our experimental apparatus and are not a fundamental limitation of the spectrogram analysis.
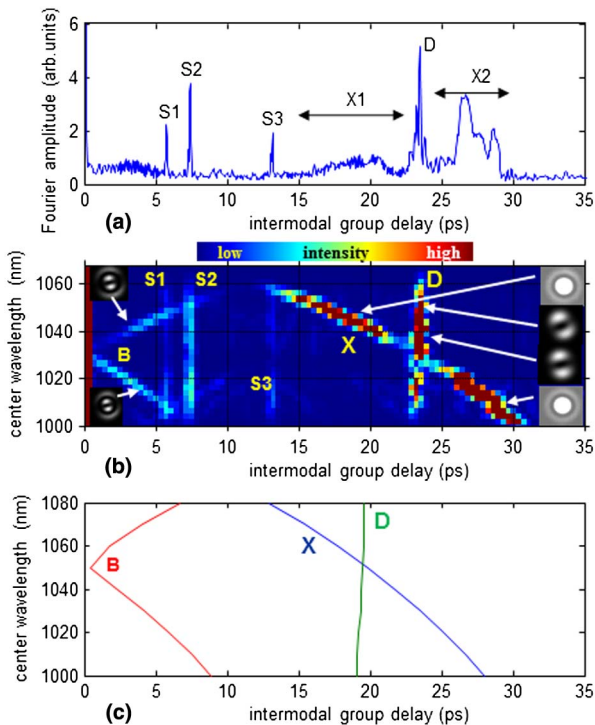

Fig. 2.   (Color online) S^2 data analysis for the LMA fiber using, (a) standard analysis [1,2], and (b) new spectrogram analysis showing a false color representation of variation in intermodal group delay as a function of wavelength. Insets in (b) show the retrieved mode intensity distribution at certain delay and wavelength values. (c) Simulated intermodal group delay as a function of wavelength.
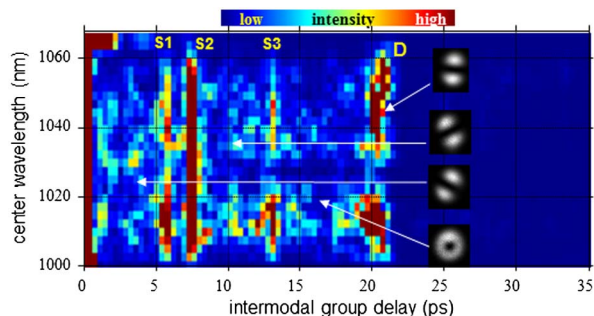
Fig. 3.   (Color online) Spectrogram recorded with the tightly coiled LMA fiber showing distributed scattering. Insets show retrieved mode images at a few representative positions.

In order to demonstrate distributed scattering, we recorded a spectrogram with the same LMA fiber coiled to a tight ~6 cm diameter (Fig. 3). The tight coil radius applies a nonaxisymmetric index perturbation that couples energy between modes all along the length of the fiber. The spectrogram shows a broad distribution of energy that extends from streak D all the way to zero intermodal group delay, independent of wavelength. Reconstruction of the mode intensity at various delays and wavelengths (Fig. 3 insets) indicates distributed scattering into the LP_{11} mode. Note that the azimuthal orientation of the LP_{11} mode shown in the insets varies more strongly compared to the discrete scattering streak D in Fig. 2(b). At some positions we observe a donut-shaped energy distribution arising from the superposition of different azimuthal orientation of LP_{11} modes. This broad distribution of energy with random mode orientation is a clear signature of distributed scattering along the entire fiber length.

We also studied a 4.3 m long standard telecom single mode fiber, which guides the LP_{01}, and LP_{11} modes at our laser wavelengths. It had some core-cladding eccentricity error, which enabled us to excite the LP_{11} mode. The standard S^2 analysis [Fig. 4(a)] shows a broad region M, which would have previously been attributed [1,2] to distributed scattering. However, our new spectrogram analysis of this data [Fig. 4(b)] shows that the intermodal group delay across feature M actually varies strongly with wavelength and therefore the delay broadening is due to mode dispersion interacting with discrete scattering into the LP_{11} mode at the input splice.

To summarize, the new two-dimensional spectrogram analysis outlined in this Letter distinguishes intermodal dispersion from distributed scattering, overcoming a
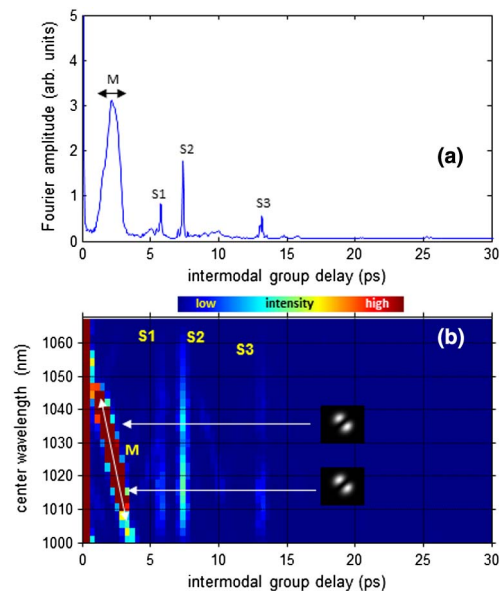

Fig. 4.   (Color online) (a) Standard S^2 analysis and (b) new spectrogram, analysis of measurements on a standard telecom single mode fiber. Insets in (b) show two representative retrieved mode images.

limitation of the standard one-dimensional representation and interpretation of S^2 data. This new approach is essential for correctly identifying the causes of intermodal scattering in fibers and for evaluating the performance of devices and systems incorporating such fibers.

References

1. J. W. Nicholson, A. D. Yablon, J. M. Fini, and M. D. Mermelstein, IEEE J. Sel. Top. Quantum Electron. **15**, 61 (2009).
2. J. W. Nicholson, A. D. Yablon, S. Ramachandran, and S. Ghalmi, Opt. Express **16**, 7233 (2008).
3. D. M. Nguyen, S. Blin, T. N. Nguyen, S. D. Le, L. Provino, M. Thual, and T. Chartier, Appl. Opt. **51**, 450 (2012).
4. D. Schimpf, R. Barankov, and S. Ramachandran, Opt. Express **19**, 13008 (2011).
5. J. Bromage, J. M. Fini, C. Dorrer, and J. D. Zuegel, Appl. Opt. **50**, 2001 (2011).
6. K. Jespersen, Z. Li, L. Nielsen, B. Palsdottir, F. Poletti, and J. Nicholson, in *Optical Fiber Communication Conference*, OSA Technical Digest (Optical Society of America, 2012), paper OTh3I.4.